A Modified Near Field Method for Measuring the Refractive Index Profile and Geometrical Parameters of Multi-Core Fibers

Ning Ma, Sujuan Huang, and Cheng Yan

***Abstract*—A modified near field (MNF) method is proposed for measuring the refractive index profile (RIP) and geometrical parameters of multi-core fibers. The near field method is based on the near field intensity at the end face of optical fibers that are illuminated by a Lambertian source to get the RIP, but the methods proposed before require a leaky-mode correction factor or additional geometrical parameters to correct the measurement results. The MNF method presented in this paper offers a simplified approach, when the power of the source is constant, the distance between the source and the incident end face of optical fibers is given, and the near field intensity distribution is linear to the RIP of the de-coated optical fibers. By using SMF-28e+ as a sample to obtain the linear coefficient, the proposed method is validated by measuring the RIP of SMF-28R with an accuracy reaching 10^{-4}. Finally, the RIP of 4-core fiber and 7-core fiber are measured by the MNF method accurately and effectively. Also, the geometrical parameters of optical fibers can be extracted through edge extraction and ellipse curve fitting for the distribution of near field intensity.**

***Index Terms*—Geometrical parameters, multi-core fiber, near field method, optical fiber measurements, refractive index profile.**

I. Introduction

With the continuous reform and innovation of Internet technology, the capacity of traditional single-mode fibers (SMFs) transmission systems can no longer meet the increasing demand for data volume [1], [2]. As a solution to the capacity limitation of current optical communication systems, multi-core fibers (MCFs) have gained significant attention because of their unique core distribution and mode field characteristics [3], [4]. MCFs are widely used not only in optical communication but also in areas such as sensors [5], measurements [6], and biological fields [7]. Accurate measurements of refractive index profile (RIP) and geometrical parameters play crucial roles in evaluating the capacity of MCFs, as they determine insertion losses, propagation modes, and bandwidths [8], [9], [10]. Therefore, developing a simple and accurate method for measuring the RIP and geometrical parameters of MCFs is essential, and it is significant for the design and optimization of MCFs, as well as for quality monitoring [11], [12], [13].

Methods for measuring parameters of optical fibers mainly are refracted near field method, digital holographic method, and microscopic technique. The refracted near field method, currently the standard method for measuring the RIP and geometric parameters of optical fibers, relies on the relationship between the refracted modes and refractive index [14], [15], [16], [17]. However, this approach demands a highly flat fiber end face and complex operational procedures. The digital holographic method is a high-precision phase imaging technique, multi-angle phase information can be captured based on the Mach-Zehnder interferometer, combining computer tomography (CT) to rebuild the RIP of optical fibers, the geometrical parameters can be extracted through the RIP [18], [19], [20], [21], [22]. However, for MCFs, the uneven distribution of cores in the cladding prevents precise measurement as the RIP becomes blurred. As for the microscopic technique, it is only suitable for measuring the geometric parameters of optical fibers [23].

The near field method was first proposed in 1976 as a means of measuring the RIP by examining the relationship between the RIP and the near field intensity at the end face of optical fibers illuminated by a Lambertian source [24]. The traditional near field method is simple, but it is only suitable for measuring the core of multimode fibers and requires a leaky-mode correction factor to obtain accurate results. Sabine et al. later modified the near field method, enabling accurate measurement of the RIP when the refractive index of the coating is lower than that of the cladding. This modification made the method suitable for both the core and cladding of multimode fibers [25], [26], [27]. Additionally, they constrained the numerical aperture (NA) of the source to be smaller than that of the optical fibers, obtaining the near field intensity of SMFs, with geometrical parameters to calculate the RIP [28].

In this paper, we present a modified near field (MNF) method for measuring the RIP and geometric parameters of MCFs. When the power of the source is constant, while the distance between the source and the incident end face of optical fibers is given,

Manuscript received 4 January 2024; revised 21 February 2024; accepted 17 March 2024. Date of publication 25 March 2024; date of current version 16 July 2024. This work was supported in part by the National Natural Science Foundation of China under Grant 62075125 and in part by the Science and Technology Commission of Shanghai Municipality under Grant 19DZ2294000. *(Corresponding author: Sujuan Huang.)*

The authors are with the Key Laboratory of Specialty Fiber Optics and Optical Access Networks, School of Communication and Information Engineering, Shanghai University, Shanghai 200444, China (e-mail: nuyoah@shu.edu.cn; sjhuang@shu.edu.cn; smartock@126.com).

Color versions of one or more figures in this article are available at https://doi.org/10.1109/JLT.2024.3380743.

Digital Object Identifier 10.1109/JLT.2024.3380743

removing the coating of the optical fibers, the near field intensity distribution is linearly related to the RIP. Take SMF-28e+ as a sample to get the linear coefficient. Then measure the RIP of SMF-28R, and compare the measurement results with S14, a commercial equipment for measuring RIP. In the end, combine the near field intensity distribution of 4-core fiber and 7-core fiber with the linear coefficient, and the RIP of 4-core fiber and 7-core fiber are obtained simply. The geometrical parameters of optical fibers can be extracted through edge extraction and ellipse curve fitting of the near field intensity distribution, and the measurement results of geometrical parameters are compared with the parameters provided by the manufacturer. The proposed method can measure the RIP and geometric parameters of MCF accurately and effectively.

II. The Modified Near Field Method

The near field method is based on measuring the near field intensity distribution at the end face of optical fibers, which is uniformly illuminated by a Lambertian source. For optical fibers with a primary protective coating that have a higher refractive index than the cladding, while the NA of the source and receiving objective is greater than that of the optical fibers. The refractive index $n(r)$ at a radius *r* from the core center is related to the near field intensity $P(r)$ by [23]:

$$\frac{n^2(r) - n_c^2}{n^2(0) - n_c^2} = \frac{P(r)}{P(0)} \frac{1}{C(r,z)} \tag{1}$$

where n_c is the cladding index value, $n(0)$ and $p(0)$ are the refractive index and intensity index at the core center respectively. The leaky-mode correction factor $C(r,z)$ is obtained by summing the Lambertian source distribution over all angles of incidence θ and azimuthal angles $\emptyset$, using a suitable weighting factor to allow the attenuation of rays, thus

$$C(r,z) = \frac{2}{\pi} \int_0^{\pi/2} d\emptyset \int \frac{\exp(-\alpha z)\, d\left(\sin^2\theta\right)}{\left[n^2(r) - n_c^2\right]} \tag{2}$$

$$0 \le \sin^2\theta \le \frac{n^2(r) - n_c^2}{\left[1 - (r/a)^2 \cos^2\emptyset\right]} \tag{3}$$

where α is the tunneling attenuation of rays launched at *r* with an angle $(\theta, \emptyset)$, z is the fiber length, and *a* is the core radius.

For optical fibers with a lower coating index than the cladding and a fiber length longer than 1 cm, there is no trace of core-edge distortion. Thus, the leaky-mode correction factor is not needed. In this case, the near field intensity $P(r)$ can be described as [24]:

$$P(r) = \frac{P(0)}{2\pi} \frac{\int_0^{\pi/2} d\emptyset \int d\left(\sin^2\theta\right)}{\left(n^2(0) - n_s^2\right)} \tag{4}$$

$$0 \le \sin^2\theta \le \frac{n^2(r) - n_s^2}{\left[1 - (r/b)^2 \cos^2\emptyset\right]} \tag{5}$$

where n_s is the coating index value, b is the cladding radius. When (4) and (5) are combined,

$$P(r) = \frac{P(0)}{\sqrt{\left\{1 - (r/b)^2\right\}}} \frac{\left[n^2(r) - n_s^2\right]}{\left(n^2(0) - n_s^2\right)} \tag{6}$$

However, in practice, larger errors occur at the edge of the cladding due to the leaky mode and the diffraction in that region [25], [26].

For SMFs, when the fiber is illuminated by a source with reduced NA [27], the coating is removed along the entire sample, exposing the cladding to air. The near field intensity in the core region is expressed as follows:

$$P(r) = P(0) \frac{n^2(r) - n_t^2}{n^2(0) - n_t^2} \tag{7}$$

where n_t is the index value of the outer layer surrounding the core. The RIP of the core can be expressed as follows:

$$n(r) = n_t + \Delta n(r) \tag{8}$$

where $\Delta n(r)$ is the difference in the RIP between the core and the outer layer surrounding the core. The near field intensity of the core can be written as:

$$p(r) = p_t + \Delta p(r) \tag{9}$$

p_t is the near field intensity of the outer layer surrounding the core, $\Delta p(r)$ is the difference in the near field intensity distribution between the core and the outer layer surrounding the core. Substituting (8) and (9) into (7), the difference in the RIP can be written as:

$$\Delta n(r) \approx \frac{n^2(0) - n_t^2}{2 n_t P(0)} \left(\Delta p(r) + p_t\right) \tag{10}$$

where p_t is close to zero. Then, (9) can be written as:

$$\Delta n(r) \approx K \times \Delta p(r) \tag{11}$$

where:

$$K = \frac{n^2(0) - n_t^2}{2 n_t P(0)} \tag{12}$$

when the power of the source remains constant, the distance between the source and the incident end face of optical fibers is given, (11) shows the near field intensity distribution is almost linear to the RIP.

III. Theoretical Simulation of the Distance Between the Source and the Incident End Face of Optical Fibers

Based on ray transmission theory, a system for the MNF method is simulated and shown in Fig. 1(a). The diameter (D) of the LED source is 1 cm, and L is the distance between the source and the incident end face of optical fibers, thus the NA of the source n_L can be defined as:

$$n_L = n_i \sin\theta_m \tag{13}$$

$$\tan\theta_m = D/2L \tag{14}$$

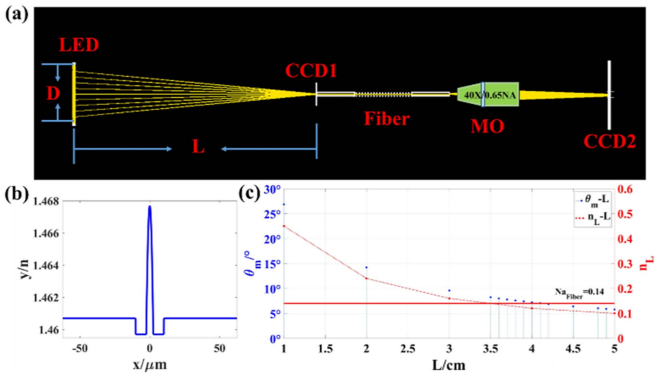

Fig. 1. Simulation of the distance between the source and the incident end face of the fiber. (a) Simulation scheme, (b) 1D RIP of the SMF, and (c) trends of θ_m and n_L following the changes in L.

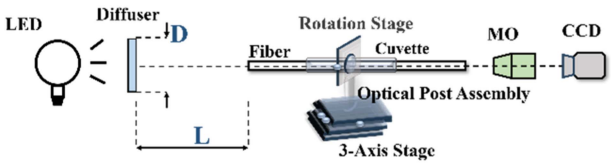

Fig. 2. Experimental equipment for the MNF method.

where n_i is the refractive index of the incidence medium and θ_m is the maximum angle of rays impinging at the end face of optical fibers. For the simulated one-dimensional (1D) RIP of the SMF shown in Fig. 1(b), the index value out of cladding is 1, and the NA of the fiber is 0.14. CCD1 is placed in front of the end face of the fiber to detect θ_m. The near field intensity profile is amplified by a microscope objective (MO) and captured by CCD2.

The NA of the source can be reduced by adjusting L. Fig. 1(c) shows the trends of θ_m and n_L following the changes in L. The results indicate that with the increase in L, θ_m and n_L both decrease. When the L value is 3.5 cm, n_L is equal to the NA of the fiber. The necessary condition to ensure that the MNF method is valid is that the NA of the source is smaller than that of the optical fibers. For this case, considering the practical size of the setup, L is chosen as 4 cm for the experimental distance and is kept constant throughout the following experiments.

IV. Experimental Verification

To validate the proposed method, an experimental setup is established, as depicted in Fig. 2. The light source is an LED with stable power. The light passes through a diffuser with a 1 cm diameter (D), which is positioned behind the LED. This diffuser ensures uniform and stable light injected into the end face of the fiber. The fiber is inserted into a cuvette and placed on a rotation stage. The rotation stage is connected to a 3-axis stage through optical post-assembly. By adjusting the 3-axis stage, the distance between the diffuser and the end face of the fiber can be adjusted. The near field intensity profile is amplified by a microscope objective (MO) with 40X and 0.75NA, captured by a 12-bit high-dynamic CCD.

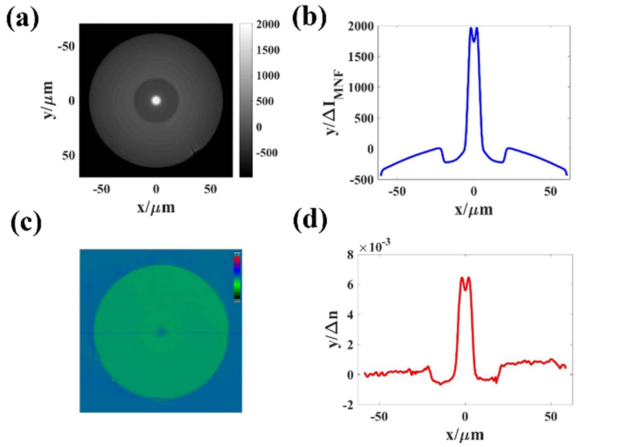

Fig. 3. Measurement results of SMF-28e+. (a) Near field intensity distribution, (b) 1D display of the near field intensity distribution, (c) normalized refracted near field intensity distribution measured by S14, and (d) 1D RIP at the solid line in (c).

A. Obtaining the Linear Coefficient Through SMF-28e+

Take SMF-28e+ with 10 cm as a sample. The entire coating is removed from the fiber, and both ends are cut flat. The fiber is inserted into the cuvette and placed on the rotation stage, which is connected to the 3-axis stage. The 3-axis stage is adjusted to ensure that the distance between the diffuser and the incident end face of the fiber is 4 cm. Turn on the LED, and the light is injected into the end face of the fiber vertically to ensure the near field intensity profile looks like a clear fiber structure image. The position of the objective is adjusted to ensure that the exit end face of the fiber aligns with the focal plane of the MO. Then the CCD records the optimal near field intensity profile amplified by MO. Fig. 3(a) shows the near field intensity profile of the SMF-28e+, its 1D display is shown in Fig. 3(b). The normalized refracted near field intensity distribution of SMF-28e+ is measured by S14, with an accuracy of 2×10^{-4}, as shown in Fig. 3(c). The solid line in Fig. 3(c) is used to obtain the 1D RIP along the cross-section, as depicted in Fig. 3(d). Additionally, S14 can measure the geometrical parameters of optical fibers, allowing for system resolution calibration based on the geometry determined by S14.

According to (11), the near field intensity distribution is almost linear to the RIP. A comparison between Fig. 3(b) and (d) illustrates the intensity distribution in the cladding region after experiencing significant distortion, confirming agreement with the aforementioned theory. Therefore, only consider the core region of the fiber. Fig. 4(a) displays the relationship between the near-field intensity distribution and the RIP of SMF-28e+, with the fit result aligning closely to the theory in a linear manner. The fitness of their relationship is represented by the black line, which has a slope of 3.4×10^{-6}, corresponding to the linear coefficient of K. The 99% confidence interval for the coefficient K is $[3.3 \times 10^{-6}, 3.5 \times 10^{-6}]$, which changes in the range of $\pm 1 \times 10^{-7}$. To evaluate the stability and reliability of the proposed method, three independent replicate experiments are performed on SMF-28e+, with sample lengths of 9.2 cm,

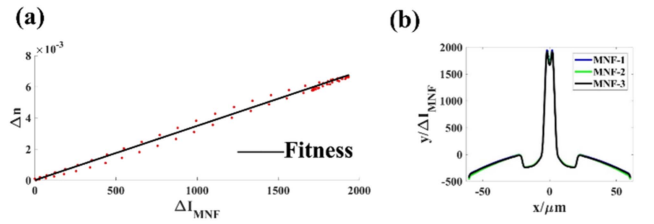

Fig. 4. (a) Relationship between the near field intensity distribution and the RIP (b) 1D near field intensity distribution of three independent replicate experiments of SMF-28e+ (marked as MNF-1, MNF-2, MNF-3).

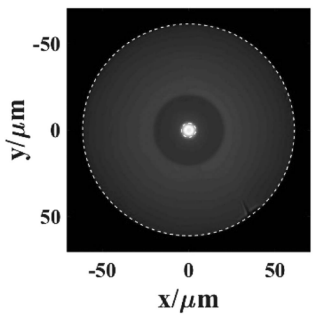

Fig. 5. Digital image processing result of Fig. 3(a).

TABLE I
COMPARISON OF THE GEOMETRICAL PARAMETERS MEASURED BY THE MNF METHOD AND PROVIDED BY THE MANUFACTURER

Parameter	Cladding diameter/ μm	Core-Cald Concentricity/ μm	Cladding Non-Circularity/ %
MNF	124.6	0.4	0.3
Manufacture	125.0±0.7	≤0.5	≤0.7

10.5 cm, and 11.2 cm. The near field intensity profile is shown in Fig. 4(b), combine the RIP measured by S14 before, refit the coefficient K three times, and the results show a good consistency with 3.4×10^{-6}. Thus, the length of optical fibers around 10 cm does not influence the fit results of coefficient K.

The digital image processing result of Fig. 3(a), achieved by edge extraction and ellipse curve fitting techniques, is presented in Fig. 5. The geometrical parameters of SMF-28e+ are obtained and compared with those provided by the manufacturer, as shown in Table I. The measurements obtained from the proposed method for the geometrical parameters fall within the specified range provided by the manufacturer.

B. Results of SMF-28R

To further validate the proposed method, SMF-28R, with a length of 10.3 cm, is chosen as a sample. The experimental conditions are kept consistent with those of SMF-28e+ mentioned earlier. Fig. 6(a) shows the near field intensity distribution of SMF-28R, while Fig. 6(b) presents the 1D display of the corresponding near field intensity distribution obtained by combining the linear coefficient from the proposed method to calculate the

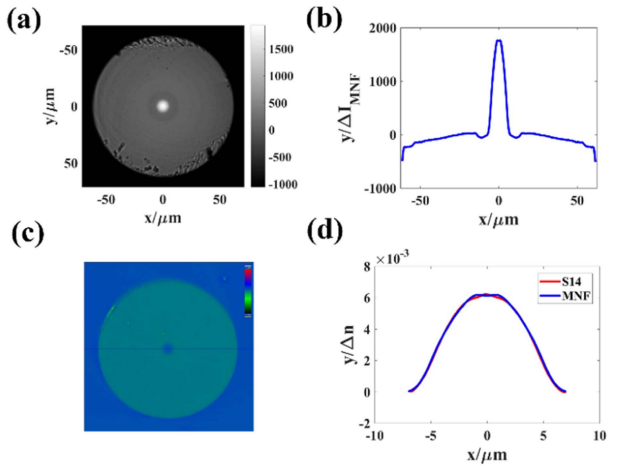

Fig. 6. Measurement results of SMF-28R. (a) Near field intensity distribution, (b) 1D display of the near field intensity distribution, (c) normalized refracted near field intensity distribution measured by S14, and (d) comparison of the RIP measurement results between the proposed method and S14.

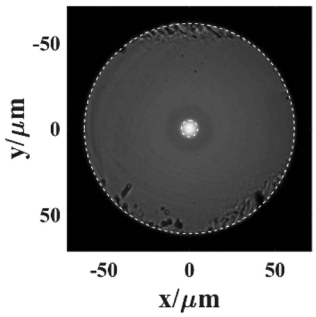

Fig. 7. Digital image processing result of Fig. 7(a).

TABLE II
MEASUREMENT RESULTS OF GEOMETRIC PARAMETERS BY THE MNF METHOD

Parameter	Cladding diameter/ μm	Core-Cald Concentricity/ μm	Cladding Non-Circularity/ %
MNF	124.3	0.3	0.3
S14	124.5	0.5	0.8

RIP of SMF-28R. Fig. 6(c) displays the normalized refracted near field intensity distribution of SMF-28R measured by S14, compared 1D RIP represented by the solid line in Fig. 7(c) with the result obtained by the MNF method are depicted in Fig. 7(d). The refractive index difference (RID) of the core measured by the MNF method is 0.0062, which is the same as the 0.0062 measured by S14. The result shows the accuracy of the proposed method for measuring the RIP of optical fibers is up to 10^{-4}.

The digital image processing result of Fig. 6(a) is shown in Fig. 7, and the extracted geometrical parameters of SMF-28R are presented in Table II. Compared to the geometrical parameters measured by S14, the cladding diameter, and core-clad concentricity are more consistent than the cladding non-circularity,

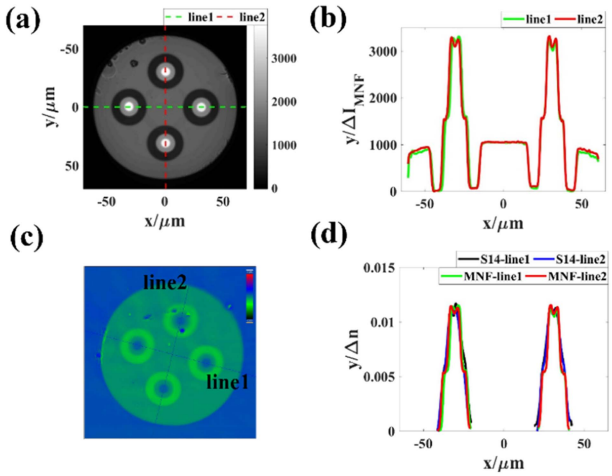

Fig. 8. Measurement results of the 4-core fiber: (a) Near field intensity distribution, (b) 1D display of the near field intensity distribution corresponding to line1 and line2 in (a), (c) normalized refracted near field intensity distribution measured by S14, and (d) 1D display of RIP corresponding to line1 and line2 in (a) and (c) (marked as MNF-line1, MNF-line2, S14-line1, and S14-line2, respectively).

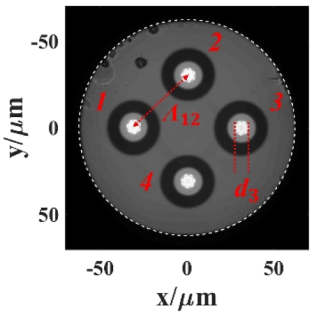

Fig. 9. Digital image processing result of Fig. 8(a).

mainly due to the lower resolution of S14 compared to the experimental setup used in this study.

C. Results of a 4-Core Fiber

The RIP and geometrical parameters of the 4-core fiber with a length of 10 cm are measured using the MNF method. The near field intensity distribution of the 4-core fiber is presented in Fig. 8(a). Fig. 8(b) displays the 1D near field intensity distribution corresponding to the dashed line labeled line1 and line2 in Fig. 8(a) respectively. When using S14 for RIP measurement of a 4-core fiber with multiple dispersive cores, obtaining the optimal refracted near field distribution of the cores in one run requires an extremely high flatness of the fiber end face, which is difficult to ensure during the complex steps involved. Consequently, measuring the RIP is quite challenging. Fig. 8(c) shows the normalized refracted near field intensity distribution of 4-core fiber measured by S14, while the RIP measurement results of two solid lines in Fig. 8(c) and two dashed lines in Fig. 8(a) are shown in Fig. 8(d).

Fig. 9 illustrates the digital image processing result of Fig. 8(a), with the cores in the fiber identified as numbers 1, 2, 3, and 4. Table III displays the RID measurement results obtained using the proposed method and S14 for each core, along with the diameter of each core. A comparison of the RID measurement results indicates that the proposed method shows more consistent results, whereas S14 produces results with a large disparity. This discrepancy is likely due to the presence of noise points in the fiber end face when measuring the refracted near field intensity using S14, as shown in Fig. 9(c). The spacings between adjacent cores are denoted Λ_{12}, Λ_{23}, Λ_{34}, and Λ_{41}. Fig. 9 shows Λ_{12} and the core diameter of core 3, which is marked d_3. The geometrical parameters of the 4-core fibers are summarized in Table IV. The data in the table reveal slight variations in the spacings between adjacent cores, all of which are approximately 44 μm. The diameter of core 2 is slightly larger than that of the other cores, possibly due to the different deformations in the fabrication of the MCF. Consequently, accurate measurements of practical geometrical parameters for optical fibers are essential.

TABLE III
MEASUREMENT RESULTS OF RID BY THE MNF METHOD AND S14

Core Number	1	2	3	4
S14	0.0116	0.0108	0.0110	0.0110
MNF	0.0113	0.0110	0.0112	0.0112

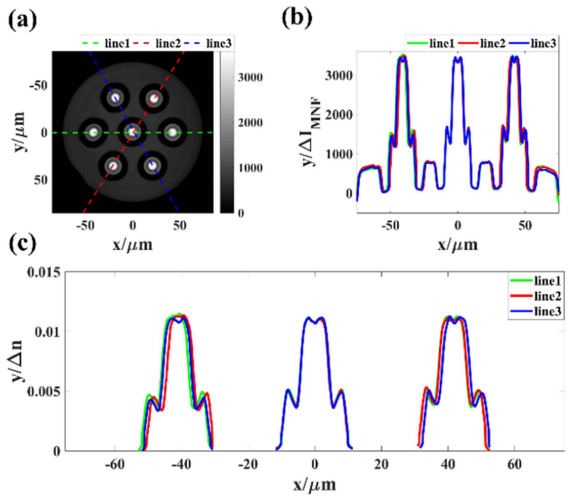

Fig. 10. Measurement results of the 7-core fiber: (a) Near field intensity distribution; (b) 1D display of the near field intensity distribution corresponding to the position of the dashed line in (a); and (c) RIP measurements corresponding to the position of the dashed line in (a).

D. Results of a 7-Core Fiber

Concerning the 7-core fibers with a greater number of cores, accurately measuring the RIP with S14 is almost impossible. In contrast, the measurement results of 7-core fiber with a length of 10 cm obtained by the proposed method are as follows. The near field intensity distribution of the 7-core fiber is shown in Fig. 10(a). Fig. 10(b) is the 1D near field intensity distribution along lines 1, 2, and 3, marked by the dashed line in Fig. 10(a). Fig. 10(c) shows the RIP measurement results corresponding to the lines in Fig. 10(a).

TABLE IV
MEASUREMENT RESULTS OF GEOMETRIC PARAMETERS BY THE MNF METHOD

Parameter	Cladding Diameter	d_1	d_2	d_3	d_4	Λ_{12}	Λ_{23}	Λ_{34}	Λ_{41}
MNF/μm	125.5	8.1	8.1	8.1	8.1	43.8	43.5	44.0	44.6

TABLE V
RID AND CORE DIAMETER MEASURED BY THE PROPOSED METHOD AND PROVIDED BY THE MANUFACTURER

Core number	0	1	2	3	4	5	6	Manufacture
RID	0.0111	0.0114	0.0111	0.0113	0.0110	0.0112	0.0112	-
Core Diameter/μm	8.2	8.2	8.1	8.1	8.1	8.1	8.1	8.0±0.5

TABLE VI
COMPARISON OF GEOMETRICAL PARAMETERS MEASURED BY THE PROPOSED METHOD AND PROVIDED BY THE MANUFACTURER

Parameter	Cladding Diameter	Λ_{01}	Λ_{02}	Λ_{03}	Λ_{04}	Λ_{05}	Λ_{06}
MNF/μm	150.2	42.6	42.0	41.3	41.4	41.8	41.3
Manufacture/μm	150.0±2.0	41.5±1.5					

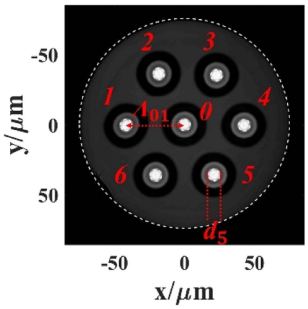

Fig. 11. Digital image processing result of Fig. 11(a).

Fig. 11 shows the results of edge extraction and ellipse curve fitting applied to the near field intensity distribution. The cores in the fiber are labeled from 0 to 6, with their respective RID and diameter detailed in Table V. Table VI provides information on the cladding diameter and the spacing between the center core and dispersive cores, which are denoted as Λ_{01}, Λ_{02}, Λ_{03}, Λ_{04}, Λ_{05}, and Λ_{06}. Fig. 11 shows Λ_{01} and the core diameter of core 5, which is marked as d_5. The measurement results in Table V indicate that the RID deviation across different cores is approximately 10^{-4}. The geometrical parameters measurement results of the proposed method, as presented in Tables V and VI, exhibit good agreement with those provided by the manufacturer. Moreover, comparing the core-to-core spacing depicted in Fig. 10(c) and Table VI, we can observe that core 3 and core 6, traversed by line 2 in Fig. 10(a), are closer to core 0, while core 1 at line 1 is further away from core 0. This observation aligns exactly with the data provided in Table VI.

V. CONCLUSION

This paper presents an MNF method for accurately and effectively measuring the RIP and geometrical parameters of MCFs. A system for SMFs is simulated based on the ray transmission theory, establishing a setup for the modified near field method to obtain the near field intensity distribution of the de-coated optical fibers. The linear coefficient between the near field intensity and the RIP is determined using SMF-28e+. By combining the near field intensity distribution with this coefficient, the final RIP of the core region in optical fibers is obtained. SMF-28R, a type of single mode fiber is measured in this paper, and those measurement results are compared with S14, which demonstrates that the proposed method for measuring the RIP achieves an accuracy of up to 10^{-4}. Furthermore, the proposed method effectively and accurately measures the RIP of the 4-core fiber and 7-core fiber. Moreover, the geometrical parameters of optical fibers can be obtained by performing edge extraction and fitting ellipse curves to the near field intensity distribution, which are in good agreement with the manufacturer. Overall, this method provides an efficient and flexible approach for measuring the RIP and geometrical parameters of MCFs which is highly important for analyzing the properties of MCFs and promoting their fabrication and application.

REFERENCES

[1] S. Tateno, H. Takeshita, K. Hosokawa, and E. L. T. de Gabory, "Capacity expansion in submarine cable systems with bidirectional transmission using 4-core-or-more MCF and MC-EDFA," *J. Lightw. Technol.*, vol. 41, no. 12, pp. 3943–3949, Jun. 2023.
[2] G. Chen, "Simulation model of AI-assisted cognitive routing algorithm for the dynamic optical network in business," *Optik*, vol. 260, 2022, Art. no. 168763.
[3] S. P. Majumder and A. Hossain, "Performance analysis of an SDM-WDM multicore optical fiber link," *Opt. Continuum*, vol. 2, pp. 600–615, 2023.
[4] L. Sun et al., "Theoretical investigations of weakly- and strongly-coupled multi-core fibers for the applications of optical submarine communications under power and fiber count limits," *Opt. Exp.*, vol. 31, pp. 4615–4629, 2023.
[5] H. Z. Du, H. Wu, Z. S. Zhang, C. Zhao, Z. Y. Zhao, and M. Tang, "Single-ended self-calibration high-accuracy Raman distributed temperature sensing based on multi-core fiber," *Opt. Exp.*, vol. 29, pp. 34762–34769, 2021.
[6] J. Cui, D. S. Gunawardena, Z. Liu, Z. Zhao, and H.-Y. Tam, "All-fiber two-dimensional inclinometer based on Bragg gratings inscribed in a seven-core multi-core fiber," *J. Lightw. Technol.*, vol. 38, no. 8, pp. 2516–2522, Apr. 2020.
[7] J. W. Sun, N. Koukourakis, J. Guck, and J. W. Czarske, "Rapid computational cell-rotation around arbitrary axes in 3D with multi-core fiber," *Biomed. Opt. Exp.*, vol. 12, pp. 3423–3437, 2021.

[8] M. Li, X. Y. Li, D. Xu, and H. Y. Li, "Performance analysis of the fiber coils combining hybrid polarization-maintaining fiber designs and symmetrical winding patterns," *Opt. Exp.*, vol. 31, pp. 22424–22443, 2023.
[9] H. T. Tong, A. Koumura, A. Nakatani, T. Suzuki, and Y. Ohishi, "Maintaining chromatic dispersion and signal gain performances in a chalcogenide buffer step-index optical fiber," *Opt. Exp.*, vol. 29, pp. 37877–37891, 2021.
[10] K. Choutagunta and J. M. Kahn, "Designing high-performance multimode fibers using refractive index optimization," *J. Lightw. Technol.*, vol. 39, no. 1, pp. 233–242, Jan. 2021.
[11] C. Wang et al., "Trench-assisted 12-core 5-LP mode fiber with a low refractive index circle and a high refractive index ring," *Opt. Exp.*, vol. 31, pp. 7290–7302, 2023.
[12] Y. Wang et al., "A novel core allocation in heterogeneous step-index multi-core fibers with standard cladding diameter," *J. Lightw. Technol.*, vol. 39, no. 22, pp. 7231–7237, Nov. 2021.
[13] T. Matsui, Y. Sagae, T. Sakamoto, and K. Nakajima, "Design and applicability of multi-core fibers with standard cladding diameter," *J. Lightw. Technol.*, vol. 38, no. 21, pp. 6065–6070, Nov. 2020.
[14] M. J. Saunders, "Optical fiber profiles using the refracted near-field technique: A comparison with other methods," *Appl. Opt.*, vol. 20, pp. 1645–1651, 1981.
[15] N. Gisin and K. W. Raine, "Correcting refracted near field refractive index profile measurements for Gaussian intensity distributions," *Opt. Commun.*, vol. 83, pp. 295–299, 1991.
[16] N. Gisin, R. Passy, and B. Perny, "Optical fiber characterization by simultaneous measurement of the transmitted and refracted near field," *J. Lightw. Technol.*, vol. 11, no. 11, pp. 1875–1883, Nov. 1993.
[17] General Administration of Quality Supervision, Inspection and Quarantine of the People's Republic of China, China National Standardization Management Committee. Specifications for optical fiber test methods-Part 20: measurement methods and test procedures for dimensions-fiber geometry: GB/T 15972.20–2008[S]. Beijing: China Standard Press, 2008. [Online]. Available: https://www.doc88.com/p-3109055373021.html
[18] H. H. Wahba, "Reconstruction of 3D refractive index profiles of PM PANDA optical fiber using digital holographic method," *Opt. Fiber Technol.*, vol. 20, pp. 520–526, 2014.
[19] C. Yan, S. Huang, Z. Miao, Z. Chang, J. Zeng, and T. Wang, "Double-cladding optical fiber's parameter measurement based on digital holographic technology," *J. Optoelectron. Laser*, vol. 27, pp. 519–527, 2016.
[20] F. Pan, Y. Deng, X. Ma, and W. Xiao, "Measurement of spatial refractive index distributions of fusion spliced optical fibers by digital holographic microtomography," *Opt. Commun.*, vol. 403, pp. 370–375, 2017.
[21] W. A. Ramadan, H. H. Wahba, M. A. S. El-Din, and I. G. A. El-Sadek, "Refractive index retrieving of polarization maintaining optical fibers," *Opt. Fiber Technol.*, vol. 40, pp. 69–75, 2018.
[22] L. Pei, Q. He, J. Wang, J. Zheng, T. Ning, and J. Li, "Complex refractive index profile measurement for special fibers using total variation method," *J. Lightw. Technol.*, vol. 41, no. 13, pp. 4097–4102, Jul. 2023.
[23] Q. He, L. Pei, T. Ning, J. Zheng, J. Li, and J. Wang, "A novel contour feature denoising method for real geometrical parameters measurement of multi-core fiber," *Opt. Fiber Technol.*, vol. 63, 2021, Art. no. 102499.
[24] S. Fme, D. N. Payne, and M. J. Adams, "Determination of optical fiber refractive index profiles by a near-field scanning technique," *Appl. Phys. Lett.*, vol. 28, pp. 255–258, 1976.
[25] D. H. Irving, F. A. Donaghy, and P. V. H. Sabine, "Fiber light acceptance for modified near field technique," *Electron. Lett.*, vol. 17, pp. 250–252, 1981.
[26] P. V. H. Sabine, D. H. Irving, and F. A. Donaghy, "Modified near-field intensity scanning of step-index fibers," *Opt. Quantum Electron.*, vol. 14, pp. 73–76, 1982.
[27] D. H. Irving, P. V. H. Sabine, and F. A. Donaghy, "A tunneling correction factor for the modified near-field technique," *Opt. Quantum Electron.*, vol. 14, pp. 17–24, 1982.
[28] D. H. Irving, "The application of near field scanning to single mode fiber profiling," *Appl. Sci. Res.*, vol. 41, pp. 325–332, 1984.

Ning Ma is currently working toward the Ph.D. degree with Shanghai University, Shanghai, China. Her main research interests include the RIP measurement of complex optical fibers and planer optical waveguides.

Sujuan Huang is currently a Professor with Shanghai University, Shanghai, China. Sujuan Huang's research interests include optoelectronic information processing and digital holographic.

Cheng Yan is currently working toward the Ph.D. degree with Shanghai University, Shanghai, China. His main research interests include the key parameters measurement of optical fibers and preforms and optical design.